Journal of Molecular Structure 1075 (2014) 486–493

Contents lists available at ScienceDirect

Journal of Molecular Structure

journal homepage: www.elsevier.com/locate/molstruc

Effect of graphene oxide on the structural and electrochemical behavior of polypyrrole deposited on cotton fabric

Fatemeh Yaghoubidoust [a], Dedy H.B. Wicaksono [b], Sheela Chandren [a], Hadi Nur [a,c,*]

[a] Ibnu Sina Institute for Fundamental Science Studies, Universiti Teknologi Malaysia, 81310 UTM Skudai, Johor, Malaysia
[b] Faculty of Biosciences and Medical Engineering, Universiti Teknologi Malaysia, 81310 UTM Skudai, Johor, Malaysia
[c] Department of Physics, Institut Sains dan Teknologi Nasional, Jl. Moh. Kahfi II, Jagakarsa, Jakarta Selatan 12640, Indonesia

HIGHLIGHTS

- Polypyrrole/graphene oxide/cotton are prepared by chemical polymerization process.
- The physical and electrochemical properties of polypyrrole/graphene oxide/cotton.
- Conductivity-physical properties relationship of polypyrrole/graphene oxide/cotton.

GRAPHICAL ABSTRACT

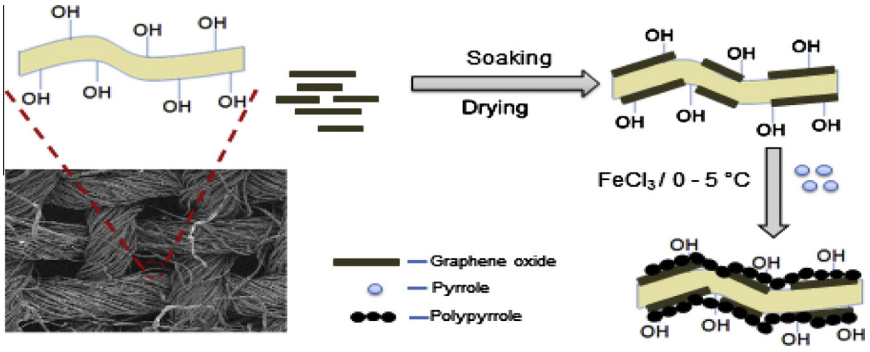

ARTICLE INFO

Article history:
Received 22 November 2013
Received in revised form 8 July 2014
Accepted 9 July 2014
Available online 16 July 2014

Keywords:
Polypyrrole
Graphene oxide
Conducting textiles
Cotton

ABSTRACT

Improving the electrical response of polypyrrole–cotton composite is the key issue in making flexible electrode with favorable mechanical strength and large capacitance. Flexible graphene oxide/cotton (GO/Cotton) composite has been prepared by dipping pristine cotton in GO ink. The composite's surface was further modified with polypyrrole (Ppy) via chemical polymerization to obtain Ppy/GO/Cotton composite. The composite was characterized using SEM, FTIR and XRD measurements, while the influence of GO in modifying the physicochemical properties of the composite was also examined using TG and cyclic voltammetry. The achieved mean particle size for Ppy/Cotton, Ppy/GO/Cotton and GO estimated using Scherrer formula are 58, 67 and 554 nm, respectively. FTIR spectra revealed prominent fundamental absorption bands in the range of 1400–1800 cm^{-1}. The increased electrical conductivity as much as 2.2×10^{-1} S cm^{-1} for Ppy/GO/Cotton composite measured by complex impedance, is attributed to the formation of continuous conducting network. The partial reduction of GO on the surface of cotton (GO/Cotton) during chemical polymerization can also affect the conductivity. This simple, economic and environmental-friendly preparation method may contribute towards the controlled growth of quality and stable Ppy/GO/Cotton composites for potential applications in microwave attenuation, energy storage system, static electric charge dissipation and electrotherapy.

Introduction

Modification of the electrical properties of cotton fibers and fabrics by incorporating conducting polymers in order to achieve exotic functional properties has been an active research domain.

* Corresponding author at: Ibnu Sina Institute for Fundamental Science Studies, Universiti Teknologi Malaysia, 81310 UTM Skudai, Johor, Malaysia. Tel.: +60 7 5536162; fax: +60 7 5536080.
E-mail address: hadi@kimia.fs.utm.my (H. Nur).
URL: http://hadinur.com (H. Nur).

http://dx.doi.org/10.1016/j.molstruc.2014.07.025
0022-2860/

Generally, conductive polypyrrole (Ppy) is chemically coated on cotton fabrics using ferric chloride as the oxidizing agent. Ppy-coated cotton fabrics are topically attractive due to their widespread applications in chemical and biological sensors [1], rechargeable batteries [2], actuators [3], light-emitting diodes [4], memory devices [5], photo-voltaic [6], corrosion resistance [7], and many more. Ppy is well known for its high electrical conductivity [8], facile preparation [9], biocompatibility and appreciable thermal stability [10]. This new generation of conductive polymers-coated fabrics is promising due to their electrical heating behavior, nonlinear optical properties, superior mechanical properties and processing advantages [11,12]. Intrinsic conducting polymers that mimic metallic conductivity, which can be achieved by the well-known approach of inserting conductive fillers into an inherently insulating resin or coating a plastic substrate with a conductive metal solution, are found to be promising [13].

Conductive fabrics can be prepared from fibers or fabrics that can be metalized with a conductive layer. The preparation methods for Ppy include chemical [12], vapor phase [14], electrochemical [15] and plasma enhanced chemical polymerization methods [16]. Chemical method offers several advantages over the other methods, such as free from contamination, simplicity, lower cost, more homogenous mixing of the components and better control over the particle size of Ppy [17,18]. The *in situ* chemical polymerization that renders relatively high conductivity is the most suitable method for dielectric coating. Methods for improving the electrical properties of such conducting polymer-coated fabrics have also been developed [19]. Additional functionality of conducting polymer-coated fabrics using triethoxysilane has also been demonstrated [20]. However, the insoluble and infusible nature of synthetic conductive Ppy restricts their processing and applications in other fields. Lately, the problem has been extensively addressed to explore applications in emerging areas.

Chemical coating of Ppy on isolated substrate has recently been developed due to their superior physical, optical and electrical properties [21]. The solution-based coating and printing techniques are intensively exploited to synthesize conductive carbon nanotubes (CNTs)-based papers and textiles for electrodes and/or current collectors in batteries and super-capacitors [22]. However, the low specific capacitance resulted from the energy storage mechanism of carbonaceous nanomaterials, limits their usage as efficient electrodes. Despite unusual and interesting properties exhibited by these CNTs-incorporated papers and textiles, the significant cost reduction for large-scale energy storage applications remains a challenge. Graphene materials, being an emerging unique class of carbon based nanoscale building blocks, possess substantial potential towards energy conversion and storage devices. Their exceptional characteristics, such as superior electronic and mechanical properties, good electrochemical stability and large specific surface area, make them viable for a variety of energy applications such as photovoltaic, batteries and super-capacitors [23]. It is commonly known that graphene acquires unique electronic band structure in the presence of Dirac point which facilitates both electron and hole to transport. This distinct band structure allows them to fabricate field-effect transistor (FET) devices with ambipolar properties [24]. Tuning of their electronic properties for electronic devices and related applications has been recently explored by different kinds of doping and also by preparing graphene nanoribbon, nanomesh and bi-layer structures [24]. Through these methods, doping of graphene is the most feasible way to control its electrical property [24]. Substitutional doping is the functionalization of graphene by covalent bonding that introduces defects into the graphene's structure. In other kinds of doping, which is basically the functionalization of graphene by non-covalent bonding, no defects are generated. Nevertheless, functionalization of graphene by covalent bonding possesses similar drawbacks to the common doping technique because defects generation decreases mobility and the on/off ratio in a graphene field-effect transistor [25]. Conversely, the non-covalent physisorption inherently driven by favorable molecular self-assembly involves dispersive interactions. This process does not remarkably modify the band structure properties, leaving the exceptional electronic structure of the graphene derivatives [25]. This strategy is predicted to be one of the keys to solve the drawbacks of common doping processes [24,25]. To date, much work has been carried out to develop GO-based nanomaterials in order to study their applications in biosensors, electronics and optoelectronics [23,26]. Based on the unique properties of GO and its derivatives, extensive efforts are dedicated to integrate GO or its derivatives into Ppy-based composite materials. In a recent study, relatively large anionic GO functions as a weak electrolyte and is captured in the Ppy composites through the electropolymerization of pyrrole, performing as an active charge-balancing dopant within the Ppy film [26]. It is proposed that the π–π interactions and hydrogen bonding between the GO layers, aromatic polypyrrole rings and the carboxyl groups of GO are efficient dopants in the polymerization. It is acknowledged that GO/Ppy composites are potential candidates for energy storage [26] and sensing application [27]. GO produced by modified Hummer's method displayed higher capacitance (as much as 189 F g^{-1}) than graphene, due to an additional pseudo-capacitance effect originated from the attached oxygen-containing functional groups on its basal planes. GO may be considered as a better electrode material than graphene in account of higher capacitance, lower cost and shorter processing time [28]. Controlled syntheses and careful characterizations of high quality stable Ppy/GO/Cotton composite with tunable structural and conducting properties have ever-growing interests in energy storage system and electronic application.

Herein, we report the preparation of high quality Ppy/GO/Cotton composite using chemical method and subsequent characterizations to examine their electroactive and conductive nature. The physicochemical and mechanical properties of these conducting fabrics are determined and compared with Ppy/Cotton composite. The mechanisms responsible for considerable improvement in conductivity and structural properties of these composites were also analyzed. The successful attachment of the solution-exfoliated GO sheets on three-dimensional, porous textiles support structures for controlled loading of active electrode materials is demonstrated. The controlled deposition of electroactive Ppy and graphene oxide nanomaterials facilitated the access of electrolytes onto the composite's structures.

Experimental

Raw materials of analytical grade such as graphite (HmbG), sulfuric acid (H_2SO_4, 97%, Grade AR, QREC), hydrochloric acid (HCl, 37%, Grade AR, QREC), ethanol (96%, Grade AR, QREC), potassium permanganate ($KMnO_4$, 99%, Sigma–Aldrich), sodium nitrate ($NaNO_3$, 99.99% Sigma–Aldrich), anhydrous sodium carbonate (Na_2CO_3, 99.9% Sigma Aldrich, USA), pyrrole (C_4H_4NH, 99.99%, Sigma–Aldrich) and iron(III) chloride ($FeCl_3$, Sigma–Aldrich) were used. GO was synthesized by modified Hummer's method [29] via chemical oxidation without further purification. The solution of GO (5 mg ml^{-1}) and deionized water was sonicated for 1 h at 100 W to form a stable dispersion. In the scouring treatment, the cotton textile was boiled for 5 min at 100 °C in deionized water. Following Nilghaz et al. [30], the first treatment was performed using 10 mg ml^{-1} anhydrous sodium carbonate. After the treatment, the samples were washed with water until the pH was reverted to the neutral range (pH = 7).

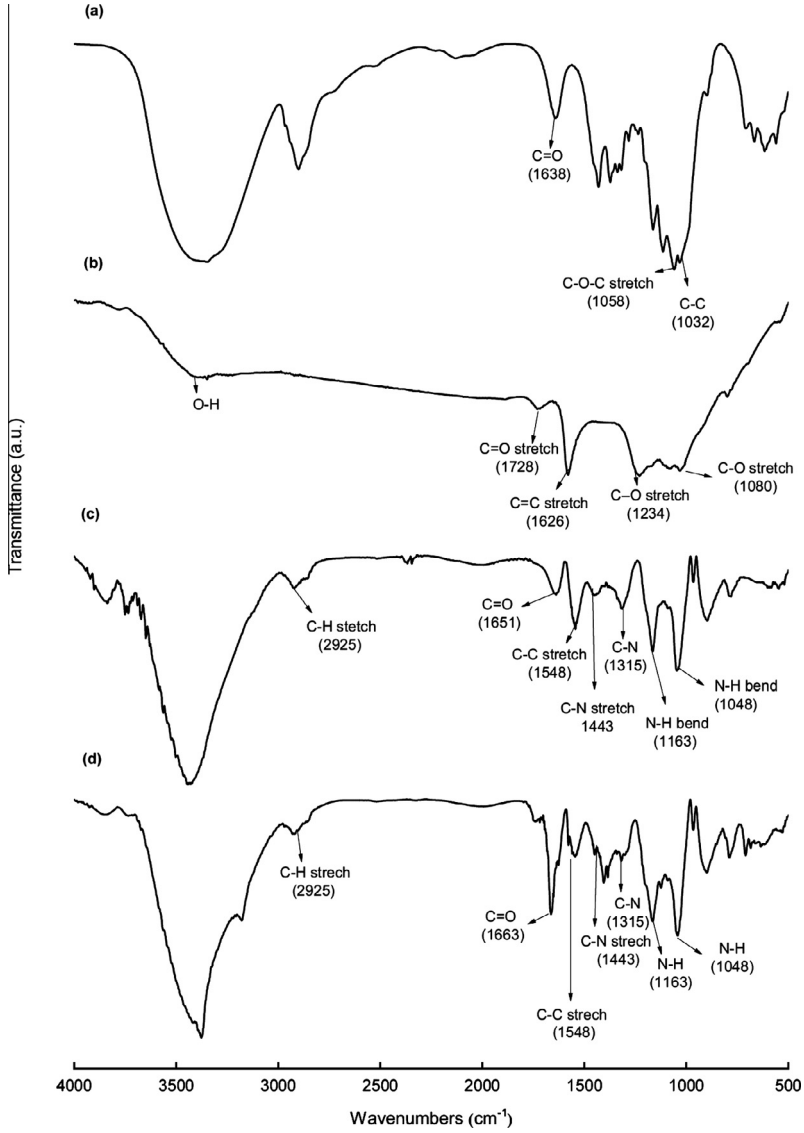

Fig. 1. FTIR spectra of (a) cotton, (b) GO, (c) Ppy/Cotton and (d) Ppy/GO/Cotton composites.

A piece of non-woven wiper cloth, with a mass density of 9.623 mg cm^{-2} and 160 fibers per inch, was used. The piece of cotton textile was dipped into the dispersed GO solution for 30 min under sonication and then dried at 80 °C for 2 h, followed by washing with deionized water and ethanol in order to remove non-attached GO. Finally, the cotton with attached graphene oxide (GO/Cotton) was dried overnight in a vacuum oven at 35 °C. The weight of GO adsorbed on the cotton textile was calculated from the difference in weight before and after attachment. Vacuum distilled pyrrole and iron(III) chloride were used for the preparation of Ppy/GO/Cotton and Ppy/Cotton. Pyrrole (0.14 ml, 2 mmol) was added to 50 ml of deionized water and GO/Cotton or pristine cotton (40 × 40 mm) that were placed in the solution and stirred for 2 h before the addition of 0.08 M $FeCl_3$ solution (50 ml) at 0–5 °C under nitrogen gas flow. The stirring was done for another 4 h. A dark layer was evident on the surface of the GO/Cotton and pristine cotton. After this treatment, the cloth samples were washed with water and ethanol until all unattached Ppy were completely removed, followed by drying in vacuum oven overnight at 35 °C. The surface resistance was measured by four-probe method. The weight of the Ppy and Ppy/GO adsorbed on the cotton was determined from the difference in weight before and after the attachment and polymerization process.

The structural characterizations were performed by X-ray diffractometer (XRD) (Bruker AXS D8 Advanced) using Cu Kα radiations (λ = 1.54178 Å) at 40 kV and 10 mA in the 2θ scanning range of 5–40°, scanning speed of ~2 min^{-1} and resolution of 0.011. Fourier transformed infrared spectroscopy (FTIR) was performed using dried KBr powder by Nexus 670 Spectrometer (Nicolet, USA). The GO ink was also characterized by transmission electron microscopy (TEM) (Tecnai G220 S-TWIN TEM, operated at 200 kV) and Raman spectroscopy (Renishaw 1000 Microspectrometer) under 532 nm excitation. Raman spectroscopy was carried out by soaking silicon substrates in graphene oxide solution (5 mg ml^{-1}) and dried in vacuum oven at 35 °C. Scanning electron microscopy (SEM) (Hitachi S-4800) was used to characterize the morphology of the as-prepared Ppy/Cotton and Ppy/GO/Cotton composites. The room temperature conductivity was measured by a DFP-02 four-point probe instrument. Four hair-thin copper wires were placed in equally spaced points in the cotton textile by using a small amount of silver paste. A steady potential was applied from a constant power supply via the two internal probes and the current across the two outermost probes was measured using a DFP-02 bench top digital multimeter [11]. Thermal stability of Ppy/Cotton and Ppy/GO/Cotton was determined by thermogravimetric analysis (TGA)

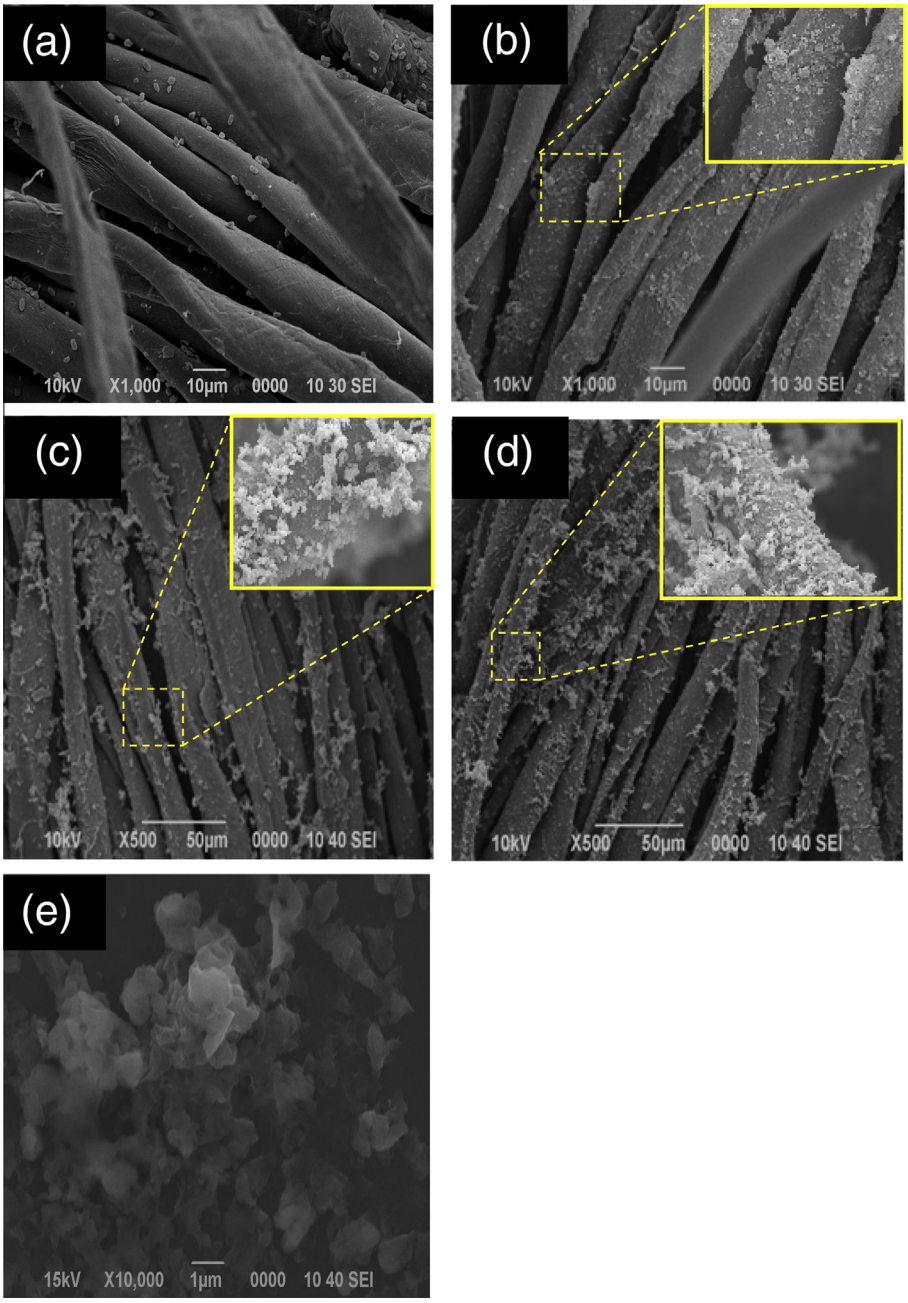

Fig. 2. SEM images of (a) pure cotton fabric, (b) GO/Cotton, (c) Ppy/Cotton, (d) Ppy/GO/Cotton composite and (e) GO.

(851 Mettler Toledo simultaneous thermal analyzer). The cyclic voltammetry (CV) and impedance measurements were carried out using potentiostat REF300017160, GAMRY 3000 Electrochemical Analyzer, USA interfaced with Gamry Echem Analyst software. In a conventional three electrodes system, Ppy/Cotton and Ppy/GO/Cotton composite (10 mm × 20 mm) were used as the working electrode for cyclic voltammetry. A platinum wire and Ag/AgCl electrode were used as the counter and reference electrodes, respectively. The test solutions were deaerated for at least 20 min with N_2 to eliminate interfering oxygen. The tensile strength was tested by Instron model 3382. All the experiments were performed at 25 ± 2 °C. The interfaced software can accurately measure impedances from 10^{10} to 0.001 Ohms, enabling electrochemical impedance spectra (EIS) EIS from 10 to 1 MHz.

Results and discussion

The FTIR spectra for cotton, GO, Ppy/Cotton and Ppy/GO/Cotton, that were recorded in the range of 400–4000 cm^1, are shown in Fig. 1. The characteristic peaks of GO; C=O stretching vibration, O—H stretching, O—H deformation vibration and aromatic C=C stretching vibration, appeared at 1728, 3404, 1395 and 1626 cm^{-1}, respectively. Meanwhile, the peaks at 1234 cm^{-1} and 1080 cm^{-1} are attributed to the epoxy C—O stretching vibration and the alkoxy C—O stretching vibration, respectively (Fig. 1b). For cotton samples, the observed absorption peak at 1548 and 1443 cm^{-1} are assigned to the C—C and C—N stretching vibrations in the pyrrole ring, respectively (Fig. 1c and d) [30,31]. The bands at 1400 and 1315 cm^{-1} are ascribed to the C—H and C—N in-plane deformation modes, respectively (Fig. 1c and d) [31,32]. The other

characteristic peaks of Ppy that can be seen at 1163 and 1048 cm^{-1} are assigned to the bending vibration for modified cotton (bipolaron modes) associated to over oxidation and N—H deformation, respectively (Fig. 1c and d) [33,34]. GO attachment caused a shift in the carboxyl peak towards a higher wavenumber from 1651 to 1663 cm^{-1} (Fig. 1d) [35]. The broad intense bands in the range of 1200 to 900 cm^{-1} are attributed to cellulose, which appeared less intense in the spectra of the modified cotton (Fig. 1a) [32]. The presence of prominent bands at 1032 and 1059 cm^{-1} are related to the functional groups of cellulose, namely the C—C, C—O and C—O—C stretching vibrations (Fig. 1a, c and d) [32]. The appearance of much weaker bands around 2850 and 3000 cm^{-1}, corresponding to the stretching of the C—H bands, confirms the attachment of Ppy on cotton fabric (Fig. 1c and d) [36].

The SEM images shown in Fig. 2b, c and d display the presence of attachment on the cotton fabric after modification. The inset of Fig. 2b shows the appearance of frequent grooves, wrinkles and roughness on the fibers' surface, verifying the successful attachment of GO nanosheets onto the cotton fiber [35]. The robust surface roughness of Ppy/Cotton and Ppy/GO/Cotton composites presented in Fig. 2c and d are due to the growth of spherical particles on the surface of pristine cotton and GO/Cotton after pyrrole polymerization. The inset of Fig. 2c and d clearly reveal the existence of these spherical particles. For reference purpose, GO flakes dispersed in deionized water by 15 min sonication and deposited on silicon substrates are given in Fig. 2e.

The TGA curves for the composites are shown in Fig. 3. A slightly lower weight loss curve is observed for Ppy/GO/Cotton than that of Ppy/Cotton due to the formation of PPy on GO layers. Furthermore, the degradation rate for Ppy/GO/Cotton composite is also lower. The initial weight loss around 100 °C is due to the removal of adsorbed water from the samples. The intermediate weight loss around 230 °C for PPy/GO/Cotton is ascribed to the decomposition of Ppy on the top of the composite. Another weight loss around 310 °C is related to the decomposition of the oxygen functional groups in GO [37,38]. Finally, the weight loss around 300 °C for Ppy/Cotton is attributed to the combustion of carbon skeleton. It is notable that the thermal decomposition temperature of Ppy/GO/Cotton composite is ~400 °C. Interestingly, the enhancement in the thermal stability of Ppy/GO/Cotton composite compared to Ppy/Cotton is due to the deposition of Ppy on GO/Cotton layers. Ppy in the Ppy/GO/Cotton composites system may have hindered the heat accumulation between GO layers. The observed weight loss for Ppy/GO/Cotton (up to 39%) and Ppy/Cotton (as much as 41%) are due to the presence of Ppy.

Fig. 4 shows the room temperature conductivities of Ppy/GO/Cotton and Ppy/Cotton composites. The conductivities, σ, were calculated using,

$$\sigma = \frac{IL}{TWV} \quad (1)$$

where L, W, T and I are the length, width, thickness of the textile samples and the current reading (mA), respectively [11]. The monotonic increase in conductivity with GO attachment is attributed to the enhanced compactness of the Ppy/GO/Cotton layer. Fabrics with attached GO and Ppy exhibit conductivities in the range of 1.12–0.90 S cm^{-1}, where the conductivity of Ppy/GO/Cotton is found to be higher than that of Ppy/Cotton composite.

The SEM images reaffirmed the attachment of GO on cotton textile. Two contributions, namely microscopic and macroscopic conductivities, are involved in the enhancement [11]. The microscopic conductivity depends on the doping level, conjugation length, chain length and many other topological factors. Conversely, the macroscopic conductivity depends primarily on external factors such as the compactness of the samples and molecular orientation. In addition, partial reduction of GO on the surface of cotton (GO/Cotton) in the presence of pyrrole as the reducing agent, may have influenced the conductivity. The conversion of pyrrole to Ppy during oxidation reaction and its subsequent adsorption on the GO/Cotton through π–π interactions affected the conductivity. Chemical polymerization of pyrrole on GO/Cotton releases electrons which are responsible for the partial reduction of GO on cotton's surface and thereby enhancing the conductivity of Ppy/GO/Cotton composite [39].

Fig. 5 illustrates the room temperature CV and impedance characteristics of the samples. 1 mol l^{-1} of Na_2SO_4 aqueous solution was used to measure the CV responses of Ppy/GO/Cotton and Ppy/Cotton composites with scanning rate of 50 mV s^{-1}. The test was performed at potential windows ranging from −0.5 to 0.5 V vs Ag/AgCl. In our three-electrode configuration, a conductive cotton textile sample was directly used as the working electrode without any mechanical support. The CV curves comparing the electrochemical behavior of Ppy/Cotton and Ppy/GO/Cotton composite displayed completely different characteristics. GO, being an insulator, limits its usage as an electrode. For the conductive fabrics attached with GO and Ppy, it is difficult to detect any redox peaks in the overall voltage range of both positive and negative sweeps [32]. Surprisingly, the larger areas of Ppy/GO/Cotton composite compared to Ppy/Cotton in the CV response are results from the electrical conductivity. At the measured scan rate, the peak current increased and the shapes of CV curves for both samples show slight distortions from an ideal capacitor. This is perhaps

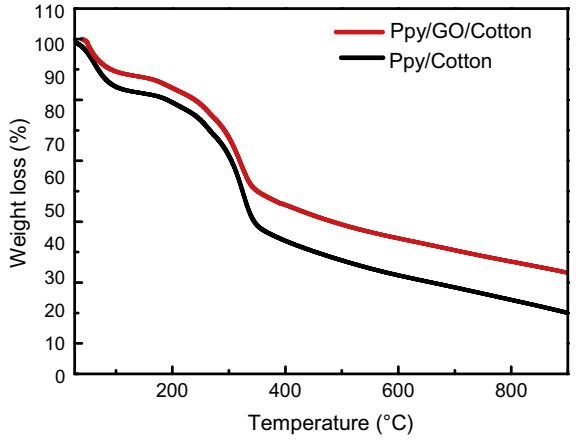

Fig. 3. TGA curves of Ppy/GO/Cotton (upper curve) and Ppy/Cotton (lower curve) composites.

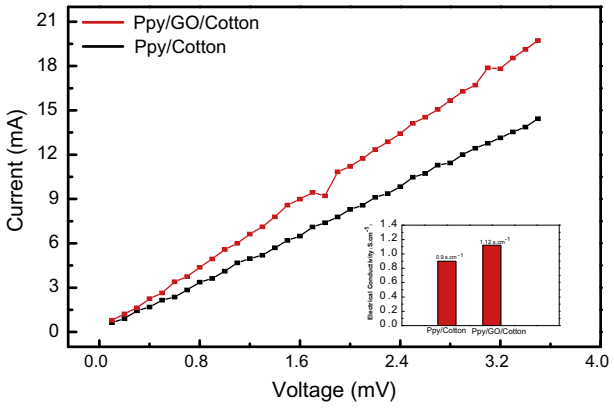

Fig. 4. The relationship between voltage and current, and conductivity measurement of polypyrrole/Cotton (PPy/Cot) and polypyrrole/ GO/Cotton (PPy/GO/Cot).

owing to increasing over-potentials from ion transport between the electrolyte and electroactive material of the composites. These higher areas exhibited by Ppy/GO/Cotton are ascribed to their different structural compactness and morphological homogeneity. The acquired electrochemical properties of Ppy/Cotton are due to the incorporation of GO originated from the alteration of oxygen functional group on its surface. This improved electrochemical feature may have immense importance in storing charge in this composite and also GO, which is known for its large surface area. Increase in the surface area of Ppy/GO/Cotton, which provided more electrode/electrolyte interface areas, led to better accessibility of electrolyte ions [28,40]. The specific capacitance, C, of Ppy/GO/Cotton and Ppy/Cotton, is calculated by the following equation:

$$C = \frac{(A/2)}{(f \times v \times m)} \tag{2}$$

where A is the integral area of the cyclic voltammogram loop, f is the scan rate, v is the voltage window and m is the mass of electroactive material. A specific capacitance of 35.7 and 24.3 F g^{-1} for Ppy/GO/Cotton and Ppy/Cotton were achieved, respectively. The capacitance achieved at a scanning rate of 50 mV s^{-1} might be comparable or lower than the reported Ppy coated nylon fabric (39.4 F g^{-1}) at the scanning rate of 100 mV s^{-1} [41].

The electrochemical impedance spectra (EIS) of Ppy/Cotton and Ppy/GO/Cotton electrodes are shown in Fig. 6, which are known as Nyquist plots. The shape of both of the spectra remains the same even after the attachment of GO on the Ppy/Cotton composite. The expected drop in equivalent series resistance (ESR) from 4.6 to 3.3 Ω of the modified fabric is consistent with the conductivity data. The observed small change in ESR at higher frequency of ~100 kHz is due to the combined resistance of the electrolyte and textile electrodes [42].

The formations Ppy/GO/Cotton and Ppy/Cotton composites are further confirmed by XRD analyses shown in Fig. 7. The XRD pattern for Ppy/Cotton comprised of four characteristic peaks centered at 14.6, 16.4, 22.6 and 34.8°, which correspond to (101), (102), (200) and (040) lattice planes, respectively, are attributed to the origin of crystalline cellulose fiber [43,44]. The crystallinity is found to reduce in Ppy-attached cotton compared to pure cotton. Amorphous Ppy peak is evident at 21°. The characteristic peak of GO, $2\theta = 10.7°$, in modified cotton fabrics (Ppy/GO/Cotton and Ppy/Cotton) is not revealed due to the very low concentration of GO loading [43]. The absence of any additional peaks related to impurities indicates the high purity of these samples. The crystallite sizes, D, are estimated from the XRD spectra using Debye–Scherrer's equation [45].

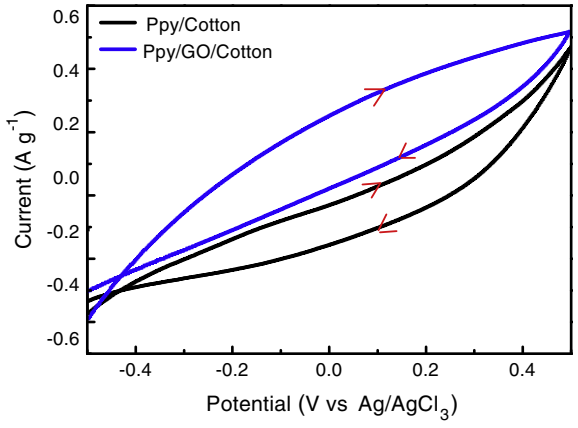

Fig. 5. CV characteristics of Ppy/Go/Cotton (upper), Ppy/Cotton (lower) in 1 mol l^{-1} of Na_2SO_4 at 50 mV s^{-1}.

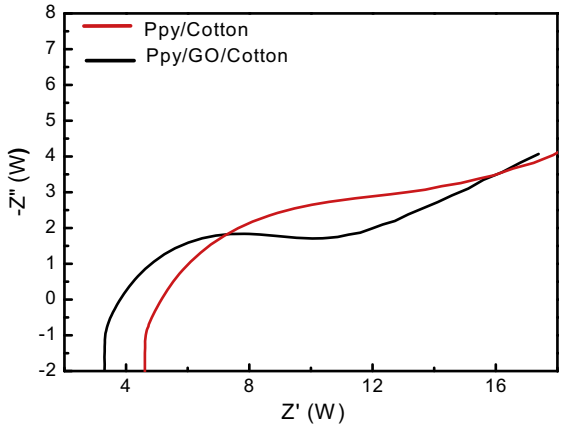

Fig. 6. Impedance curves of Ppy/Cotton (red) and Ppy/GO/Cotton (black) with Z' (real impedance) and Z'' (imaginary impedance). (For interpretation of the references to colour in this figure legend, the reader is referred to the web version of this article.)

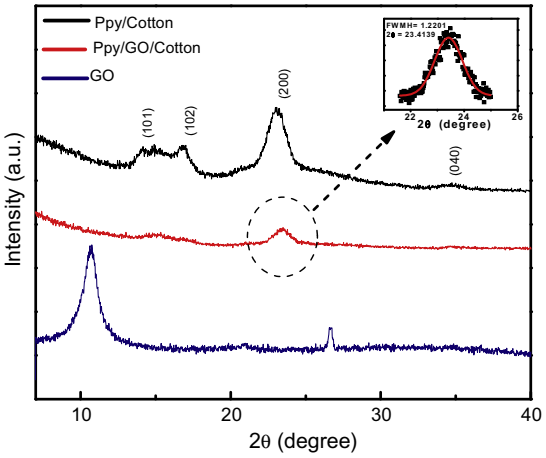

Fig. 7. XRD patterns for Ppy/Cotton, GO and Ppy/GO/Cotton composites.

$$D = \frac{k\lambda}{\beta \cos\theta} \tag{3}$$

where λ is the wavelength of the X-ray radiation, K is a constant taken as 0.89, β is the full width at half maximum (FWHM) of line broadening and θ is the angle of diffraction. The most intense peak was used to estimate the sizes of Ppy/Cotton, Ppy/GO/Cotton and GO, which are found to be 63, 77 and 554 nm, respectively. The average particle size of Ppy/GO/Cotton is similar to Ppy/Cotton with very low concentration of GO loading, showing no significant change after the attachment of GO.

The TEM image of GO shown in Fig. 8a clearly displays the formation of large flakes. The presence of a typical amorphous ring in the selected angle electron diffraction (SAED) pattern (inset of Fig. 8b) indicates that the GO is amorphous in nature. However, in the XRD pattern of GO (Fig. 7) some peaks are detected indicating that the sample contains crystalline phase [46].

Raman spectroscopy is a widely used tool for characterizing carbon products, which render elevated intensities for conjugated and double carbon–carbon bonds [47]. In the solitary previous computational study of Raman spectra, oxidized nanotubes are modeled as relatively shorter hydrogen terminated nanotube segments. This geometry introduces spurious features into the vibrational modes and offers a major challenge in interpreting experimental data. The infrared spectra of various finite graphitic structures with edge

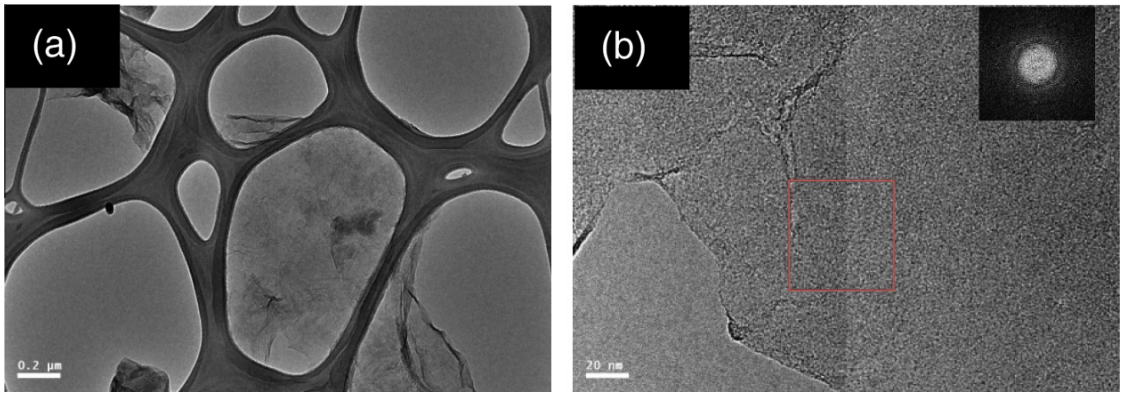

Fig. 8. (a) TEM and (b) SAED images of GO sample.

groups are also calculated. However, for most models on GO that involve intact hexagonal carbon lattice, the placement of chemical groups are random throughout the two dimensional (2D) sheet without putting on the edges and require accurate modeling of the GO structure. The Raman spectrum of GO is shown in Fig. 9. The spectrum reveals intense D and G bands centered at 1274 and 1543 cm^{-1}, respectively with $I_D/I_G = 0.97$ (I_D is the intensity of D band and I_G is the intensity of G band) and a flat 2D region, which are in conformity with literature [46–48]. The appearance of silicon peak at 449.8 cm^{-1} is the effect of the silicon substrate. The observed G band and D band indicate the reduction in size of the in-plane sp^2 domains, which is caused by extensive oxidation, indicating the successful oxidation of graphite flakes. These two main prominent peaks for GO are dependent on the laser excitation, that is E_{2g} vibrational mode in-plane and A_{1g} breathing mode, respectively. G band is Raman active for sp^2 hybridized carbon-based material, whereas D band only appears if defects participate in the double resonance Raman scattering near *K* point of Brillouin zone. The intensity ratio of I_D/I_G is used for estimating the sp^2 domain size of graphite-based materials [49,50].

The samples were cut into pieces with a dimension of 15 × 80 mm. Retaining the mechanical stability of textiles during the coating process is critically significant for practical applications. Textile performance of the modified cotton fabrics is valued in terms of their mechanical features. Tensile strengths of the original cotton, GO/Cotton, Ppy/Cotton and Ppy/GO/Cotton fabrics are measured and summarized in Table 1. In comparison with the original cotton, the tensile strength was enhanced when GO is attached onto the cotton textile and then decreases as Ppy was further added on. The maximum tensile strength of GO/Cotton composite increased by 142% (0.038 to 0.054 kN). The high strength must be owing to the good interaction between the cellulose's chains and the GO flakes. The hydroxyl and carboxyl functional groups on the GO are applicable to make strong interactions with the hydroxyl groups on the cellulose's structure. This provides

Table 1
Tensile strength of cotton, GO/Cotton, Ppy/Cotton and Ppy/GO/Cotton.

Sample	Tensile strength (kN)
Cotton	0.038
GO/Cotton	0.054
Ppy/Cotton	0.017
Ppy/GO/Cotton	0.035

better interaction between the cellulose matrix and GO [51]. The influence of *in situ* polymerization of pyrrole on the maximum tensile strength for cotton textile has been measured with 44% reduction (0.38 to 0.17 kN). The loss of tensile strength for Ppy/Cotton can be caused by the non-flexible origin of Ppy attached on the cellulose's structure, which limits the contribution of the fiber to fiber cohesion. The oxidative decay of cotton might have also played a part as ferric chloride is a strong oxidant [52]. It is further demonstrated that the attachment of GO on the cotton fabric has improved the construction of cotton fibers. However, pyrrole chemical polymerization decreased the tensile strength of the cotton fibers, which was compensated by the attachment of GO. This supports the suitability of Ppy/GO/Cotton composites for sundry practical applications.

Conclusion

Ppy/GO/Cotton composites were successfully synthesized via the economic yet accurate chemical polymerization method. The role of GO in altering the structural, physical and electrochemical properties was studied through in-depth characterizations at room temperature. The presence of GO is found to increase the electrical conductivity of Ppy/GO/Cotton composite by forming continuous conducting network. The existence of GO and the formation of the composite were confirmed by XRD pattern and Raman spectra. The SEM images further confirmed the attachment of GO on the

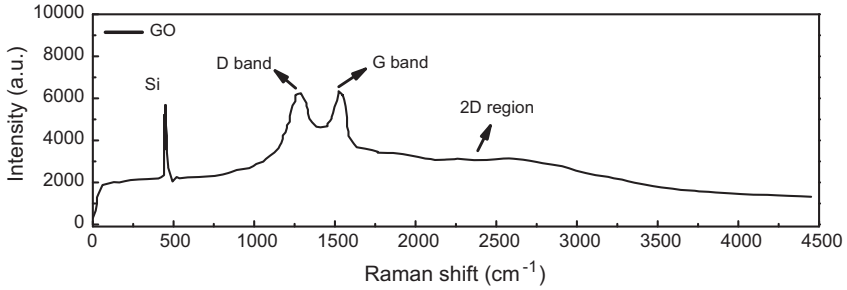

Fig. 9. Raman spectrum of GO under 514 nm excitation.

composites. The enhanced compactness of the Ppy/GO/Cotton layer by the attachment of GO increased the room temperature conductivities of Ppy/GO/Cotton and Ppy/Cotton composites. The structural compactness and outstanding homogeneity of Ppy/GO/Cotton composite imparted higher CV response than Ppy/Cotton sample. The mechanical properties of the composite are similar to those of the original cotton. The outstanding features of the results indicate that this easy and environmental-friendly preparation method may constitute a basis for producing stable Ppy/GO/Cotton composites in a controlled fashion which is viable for device fabrication.

Acknowledgments

The authors gratefully acknowledge funding by the Ministry of Higher Education (MOHE), Malaysia through Fundamental Research Grant Scheme and Universiti Teknologi Malaysia through Research University Grant. The authors also would like to thank Ali A. Ati (Ibnu Sina Institute for Fundamental Science Studies, UTM) for his help in the electrical conductivity measurement.

References

[1] Q. Li, C. Zhang, Z. Xue, J. Li, Chin. J. Chem. Phys. 23 (2010) 207–210.
[2] H. Song, G.T.R. Palmore, Adv. Mater. 18 (2006) 1764–1768.
[3] Y. Berdichevsky, Y. Lo, Adv. Mater. 18 (2006) 122–125.
[4] J. Gao, A.J. Heeger, J.Y. Lee u, C.Y. Kim, Synth. Met. 82 (1996) 221–223.
[5] S. Barman, F. Deng, R.L. McCreery, J. Am. Chem. Soc. 130 (2008) 11073–11081.
[6] A.A. Stefopoulos, C.L. Chochos, M. Prato, G. Pistolis, K. Papagelis, F. Petraki, S. Kennou, J.K. Kallitsis, Chem. Eur. J. 14 (2008) 8715–8724.
[7] E. Hermelin, J. Petitjean, J. Lacroix, K.I. Chane-Ching, J. Tanguy, P. Lacaze, Chem. Mater. 20 (2008) 4447–4456.
[8] T.K. VishnuvArdhan, V.R. Kulkarni, C. Basavaraja, S.C. Raghavendra, Bull. Mater. Sci. 29 (2006) 77–83.
[9] W. Aimei, H. Kolla, S.K. Manohar, Macromolecules 38 (2005) 7873–7875.
[10] K. Vahidi, Y.S. Jalili, J. Theor. Appl. Phys. 7 (2013) 1–9.
[11] A.C. Macasaquit, C.A. Binag, Philippine J. Sci. 139 (2010) 189–196.
[12] R.E. Myers, J. Electron. Mater. 15 (1986) 61–69.
[13] A.C. Sparavigna, L. Florio, J. Avloni, A. Henn, Mater. Sci. Appl. 1 (2010) 253–259.
[14] D.S. Jinyeol Kim, Y. Sung, E.R Kim, Synth. Met. 132 (2003) 309–313.
[15] M. Takakubo, Synth. Met. 16 (1987) 167–172.
[16] K. Hosono, I. Matsubara, N. Murayama, W. Shin, N. Izu, Mater. Lett. 58 (2004) 1371–1374.
[17] X. Zhang, J. Zhang, W. Song, Z. Liu, J. Phys. Chem. B 110 (2006) 1158–1165.
[18] Y. Kudoh, K. Akami, Y. Matsuya, Synth. Met. 95 (1998) 191–196.
[19] E. Håkansson, A. Amiet, A. Kaynak, Synth. Met. 157 (2007) 1054–1063.
[20] M. Katarína, M.M. Chehimi, P. Fedorko, M. Omastová, Chem. Pap. 67 (2013) 979–994.
[21] M. Ferenets, A. Harlin, Thin Solid Films 515 (2007) 5324–5328.
[22] L. Hu, M. Pasta, F. Mantia, L. Cui, S. Jeong, H. Deshazer, J. Choi, S. Han, Y. Cui, Nano. Lett. 10 (2010) 708–714.
[23] J. Liu, Y. Xue, M. Zhang, L. Dai, MRS Bull. 37 (2012) 1265–1272.
[24] A. Jang, E. Jeon, D. Kang, G. Kim, B. Kim, H.S. Shin, ACS Nano 6 (2012) 9207–9213.
[25] B. M Wong, H. Ye Simon, G. O'Bryan, Nanoscale 4 (2012) 1321–1327.
[26] C. Zhu, J. Zhai, D. Wen, S. Dong, J. Mater. Chem. 22 (2012) 6300–6306.
[27] J.W. Park, S.J. Park, O.S. Kwon, C. Lee, J. Jang, Anal. Chem. 86 (2014) 1822–1828.
[28] B. Xu, S. Yue, Z. Sui, X. Zhang, S. Hou, G. Cao, Y. Yang, Energy Environ. Sci. 4 (2011) 2826–2830.
[29] J.W.S. Hummers, R.E. Offeman, J. Am. Chem. Soc. 80 (1958). 1339–1339.
[30] A. Nilghaz, D.H.B. Wicaksono, D. Gustiono, F.A.A. Majid, E. Supriyanto, M.R.A. Kadir, Lab. Chip. 12 (2012) 209–218.
[31] M. Omastova, M. Trchova, J. Kovářová, J. Stejskal, Synth. Met. 138 (2003) 447–455.
[32] G. Liang, L. Zhu, J. Xu, D. Fang, Z. Bai, W. Xu, Electrochim. Acta 103 (2013) 9–14.
[33] K.S. Jang, H. Lee, B. Moon, Synth. Met. 143 (2004) 289–294.
[34] I. Rodríguez, B.R. Scharifker, J. Mostany, J. Electroanal. Chem. 491 (2000) 117–125.
[35] K. Krishnamoorthy, U. Navaneethaiyer, R. Mohan, J. Lee, S. Kim, Appl. Nanosci. 2 (2012) 119–126.
[36] R.G. Snyder, S.L. Hsut, S. Krimm, Spectrochim. Acta A 34 (1978) 395–406.
[37] S. Konwer, R. Boruah, S.K. Dolui, J. Electron. Mater. 40 (2011) 2248–2255.
[38] Y. S Lim, Y.P. Tan, H.N. Lim, W.T. Tan, M.A. Mahnaz, Z.A. Talib, N.M. Huang, A. Kassim, M.A. Yarmo, J. Appl. Sci. 128 (2013) 224–229.
[39] C.A. Amarnath, C.E. Hong, N.H. Kim, B. Ku, T. Kuila, J.H. Lee, Carbon 49 (2011) 3497–3502.
[40] Y. S Lim, Y.P. Tan, H.N. Lim, N.M. Huang, W.T. Tan, J. Polym. Res. 20 (2013) 1–10.
[41] B. Yue, C. Wang, X. Ding, G.G. Wallace, Electrochim. Acta 68 (2012) 18–24.
[42] K.F. Babu, R. Senthilkumar, M. Noel, M.A. Kulandainathan, Synth. Met. 159 (2009) 1353–1358.
[43] K.F. Babu, P. Dhandapani, S. Maruthamuthu, M.A. Kulandainathan, Carbohyd. Polym. 90 (2012) 1557–1563.
[44] J. Zhao, B. Deng, M. Lv, J. Li, Y. Zhang, H. Jiang, C. Peng, J. Li, J. Shi, Q. Huang, C. Fan, Adv. Healthcare Mater. 2 (2013) 1259–1266.
[45] A.A. Ati, Z. Othaman, A. Samavati, F. Yaghoubidoust, J. Mol. Struct. 1058 (2014) 136–141.
[46] D. Chen, L. Li, L. Guo, Nanotechnology 22 (2011) 325601.
[47] Y. Wang, D.C. Alsmeyer, R.L. McCreery, Chem. Mater. 2 (1990) 557–563.
[48] K.N. Kudin, B. Ozbas, H.C. Schniepp, R.K. Prud'Homme, I.A. Aksay, R. Car, Nano Lett. 8 (2008) 36–41.
[49] D. Zhan, Z. Ni, W. Chen, L. Sun, Z. Luo, L. Lai, T. Yu, A.T.S. Wee, Z. Shen, Carbon 49 (2011) 1362–1366.
[50] S. Stankovich, D.A. Dikin, R.D. Piner, K.A. Kohlhaas, A. Kleinhammes, Y. Jia, Y. Wu, S.T. Nguyen, R.S. Ruoff, Carbon 45 (2007) 1558–1565.
[51] L. Zhang, Z. Wang, C. Xu, Y. Li, J. Gao, W. Wang, Y. Liu, J. Mater. Chem. 21 (2011) 10399–10406.
[52] A.J. Patil, A.K. Pandey, Indian J. Fibre Text. Res. 37 (2012) 107–113.